Research Article

Achieving zero thermal expansion over a wide temperature range in (Hf,Ta)(Fe,Cr)$_2$ alloys

Xiaobo Wang[1]; Minjun Ai[1,#]; Feixiang Long[1]; Hong Zhong[1]; Hao Lu[1]; Jun Chen[1,*]; Chang Zhou[2,*]

[1]Beijing Advanced Innovation Center for Materials Genome Engineering, Department of Physical Chemistry, University of Science and Technology Beijing, Beijing, 100083, China

[2]State Key Laboratory for Advanced Metals and Materials, University of Science and Technology Beijing, Beijing, 100083, China

Correspondence to: Jun Chen, Beijing Advanced Innovation Center for Materials Genome Engineering, Department of Physical Chemistry, University of Science and Technology Beijing, Beijing, 100083, China. E-mail: junchen@ustb.edu.cn

Abstract

Zero thermal expansion alloys possess significant potential for applications in aerospace, electronics, and optical instruments due to their volume remains nearly constant despite temperature changes[1,2,3]. Regulating and exploring zero thermal expansion alloys is crucial to mitigating thermal strain and stress. This study successfully adjusted negative thermal expansion alloy (Hf, Ta)Fe$_2$ to zero thermal expansion over a wide temperature range by optimizing its composition and controlling the magnetic phase transition.

Moderately substituting Cr for Fe transformed the giant negative thermal expansion (ΔT=15 K) into zero thermal expansion (ΔT=260 K). High-resolution synchrotron X-ray diffraction, macroscopic magnetic measurements, and linear thermal expansion measurements were employed to investigate the crystalline structures, magnetic properties, and thermal expansion of $Hf_{0.84}Ta_{0.16}Fe_{2-x}Cr_x$ ($0 \leq x \leq 0.25$). The alignment of the magnetic phase transition and anomalous thermal expansion temperature ranges demonstrates the essential role of spin-lattice coupling[4]. This work offers valuable insights into regulating zero thermal expansion behavior and explaining the applications of magnetic negative thermal expansion alloys. This advancement will promote their use in high-precision instruments, aerospace, microelectronics, and advanced manufacturing, enhancing device reliability and performance, particularly in extreme temperature environments[5,6].

INTRODUCTION

Zero thermal expansion (ZTE) is a rare and precious property where the material exhibits negligible volume change with increasing temperature[7,8]. ZTE occurs when the contraction of at least one dimension of the material with rising temperature compensates for the positive thermal expansion (PTE), resulting in negligible volume change[9,10]. This anomalous behavior has attracted considerable research interest, providing a basis for understanding the physical nature of thermal expansion, and leading to the development of a new class of functional materials with unique practical value[11,12]. Research on anomalous thermal expansion dates back to 1897, when Guillaume first discovered zero thermal expansion in Invar alloys[13]. This alloy series, along with the later discovered magnetic negative thermal expansion (NTE) alloys, has been essential in aerospace remote sensors, high-pressure compressor casings, frequency generators, and printed circuit boards, due to their ability to compensate for

PTE and their excellent thermal conductivity[14,15,16]. Magnetic NTE alloys can also be tuned into ZTE alloys directly. Developing high-performance ZTE alloys requires significant effort, and their practicality is often limited by narrow working temperature ranges[17,18]. Thus, regulating the magnetism and temperature range of NTE alloys is crucial for enhancing their versatility and applicability, maximizing their potential in various technological applications[19,20].

Chemical substitution is one of the most effective methods for regulating thermal expansion in NTE materials. It affects thermal expansion by introducing defects and stress, and altering the material's magnetism[21]. For instance, Song et al. achieved ZTE in $TbCo_2$ by substituting Fe in the Co sublattice[22]. Similarly, Huang et al. Incorporated Co into $La(Fe, Si)_{13}$ to expand its NTE temperature range and broadening the temperature window in $La(Fe, Co, Si)_{13}$[23]. Additionally, Xu et al. employed the method of interstitial atom doping. They achieved zero thermal expansion in $La(Fe, Si)_{13}$ by doping hydrogen atoms into the lattice[24]. Xu et al. regulated $HfFe_2$ by changing the non-stoichiometric ratio and successfully broadened its negative thermal expansion temperature window[25]. In addition to these traditional methods, some novel approaches have also been put forward. For instance, Yuan et al. broadened the NTE temperature range of Mn_3GaN by means of increasing the configurational entropy of Ga-site[26]. Xu et al. modulated the thermal expansion coefficient of PTE $HfFe_2$ to 1.25×10^{-6} K^{-1} in the temperature range of 433 – 583 K through non-stoichiometric engineering. Regulating PTE to ZTE or NTE is highly meaningful, and various attempts have been made to realize ZTE or NTE in the $HfFe_2$ series[25]. Song et al. presented the coexistence of ferromagnetic NTE phase and paramagnetic PTE phase via chemical substitution of Hf by Nb and attained ZTE $(Hf, Nb)Fe_2$[27]. Li et al. used Ta to substitute and obtained $(Hf, Ta)Fe_2$ with NTE performance. When the temperature is between 222 – 327 K, the thermal expansion coefficient reaches -16.3×10^{-6} K^{-1}, making it a very promising NTE material[28]. However, the large NTE of $(Hf, Ta)Fe_2$ caused by a first-order magnetic phase transition, is difficult to regulate to ZTE, especially due to the narrow and low

temperature range. Therefore, the regulation of thermal expansion of $(Hf, Ta)Fe_2$ has become a focus of research aiming to fully exploit its application potential[29,30,31].

Herein, ZTE in $Hf_{0.84}Ta_{0.16}Fe_{1.9}Cr_{0.1}$ at room temperature was achieved by moderately substituting Fe with Cr. We successfully broadened the temperature range to 110 - 370 K with a CTE of 1.55×10^{-6} K^{-1}. By refining the synchrotron X-ray diffraction profiles and analyzing the magnetic data and the thermal expansion data, it can be concluded that the thermal expansion of $(Hf, Ta) Fe_2$ is primarily governed by the magnetism of Fe(6h). Cr substitution alters the Fe–Fe pair spacing, weakening the magnetic interaction and reducing the interaction between iron atom[32]. The reduced interaction between iron atoms weakens the negative thermal expansion trend, and the slow down in this process results in the emergence of ZTE. This is beneficial to broaden the NTE temperature window of $(Hf, Ta)Fe_2$.

EXPERIMENTAL

A series of $Hf_{0.84}Ta_{0.16}Fe_{2-x}Cr_x$ ($0 \leq x \leq 0.25$) samples were all melted in an arc furnace under a high-purity argon atmosphere. The raw materials were all high-purity metals of Hf, Ta, Fe, and Cr with a purity of 99.99%. To ensure the uniformity of the ingots, the melting operation was repeated 4 - 5 times for each ingot. During each melting process, the ingot was turned over. After the melting process was completed, the ingot was wrapped with molybdenum foil and sealed in a vacuum-tight quartz tube, and then annealed in a muffle furnace at 1223 K for 5 days before being slowly cooled down to room temperature. In addition, high-resolution synchrotron X-ray diffraction (SXRD) patterns were collected on the BL02B2 beamline at SPring-8. The phase composition and crystal structure were analyzed, and the X-ray diffraction (XRD) patterns were refined using Fullprof program. All the thermal expansion data of the samples were obtained using a NETZSCH thermomechanical analyzer with a heating rate of 5 K/min. To better analyze the regulation mechanisms, the macroscopic magnetic properties of the samples were measured using the Quantum Design Physical Property Measurement

System (PPMS) and the Vibrating Sample Magnetometer (VSM).

RESULTS AND DISCUSSION

The XRD patterns of $Hf_{0.84}Ta_{0.16}Fe_{2-x}Cr_x$ ($0 \leq x \leq 0.25$) are shown in Figure 1a. The temperature-dependent XRD data for $Hf_{0.84}Ta_{0.16}Fe_2$ was collected and refined using the Rietveld method (Figure 1b). In this study, based on the diffraction XRD data obtained under the condition of room temperature (300 K) and the corresponding refined results of $Hf_{0.84}Ta_{0.16}Fe_2$, we thoroughly analyzed its crystal structure (Figure 1c). In $Hf_{0.84}Ta_{0.16}Fe_2$, Hf atoms and Ta atoms are mixed with each other and jointly occupy the Wyckoff site 4f with coordinates of (1/3, 2/3, z). Meanwhile, Fe atoms are distributed in two different Wyckoff sites, namely 2a (0, 0, 0) and 6h (x, 2x, 1/4)[33]. It is particularly noteworthy that the iron atoms located at the 6h site are arranged in the ab plane to form a unique two-dimensional kagome structure, and it is reported that this structural feature is related to the regulation of NTE through magnetic phase competition[34]. To further explore the thermal expansion characteristics of the $Hf_{0.84}Ta_{0.16}Fe_{2-x}Cr_x$, we conducted systematic tests on their macroscopic linear thermal expansion (Figure 1d). The results showed that in the undoped state, $Hf_{0.84}Ta_{0.16}Fe_2$ exhibited a very significant NTE phenomenon. However, as the Cr element was gradually incorporated, an interesting phenomenon occurred: the negative thermal expansion trend gradually became gentler. Correspondingly, the thermal expansion coefficient steadily increased, and the working temperature window was also broadened. It is especially worth mentioning that when the Cr content reached 0.1, the linear thermal expansion characteristics of the material exhibited an excellent performance of ZTE. At this time, for $Hf_{0.84}Ta_{0.16}Fe_{1.9}Cr_{0.1}$, the zero thermal expansion temperature range extended to 110 K to 370 K, and the thermal expansion coefficient was as low as only $1.55 \times 10^{-6} K^{-1}$. The previously reported $Hf_{0.85}Ta_{0.15}Fe_2C_{0.01}$ by Xu et al. also exhibits the ZTE phenomenon with a thermal expansion coefficient of 2.4×10^{-6} K^{-1}, but the ZTE occurs at a low temperature[35]. Moreover, Xu et al. also regulated $HfFe_{2+\delta}$ through the non-stoichiometric methodology to achieve a thermal expansion coefficient of 1.25×10^{-6} K^{-1}, but the only drawback is

that the temperature operating window also does not include room temperature[25]. Therefore, our remarkable thermal expansion regulation effects demonstrate a great success and further exploit the potential of this material system in practical applications[36].
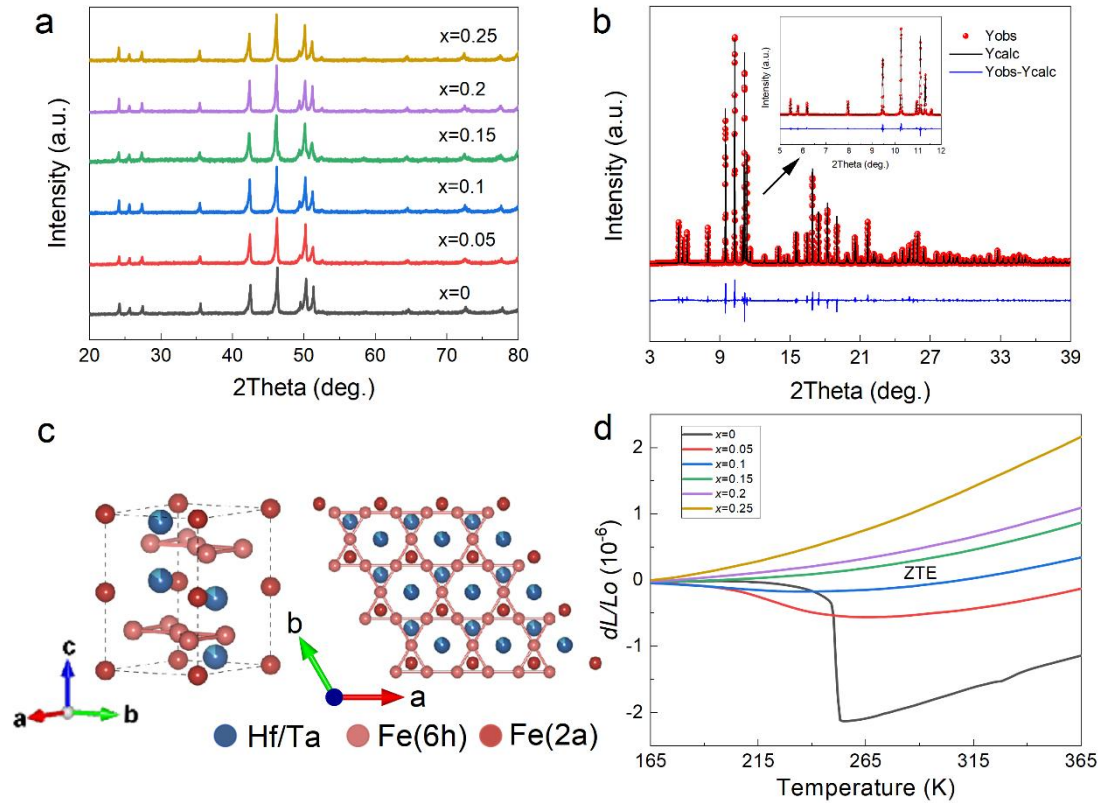
Figure 1. (a) XRD patterns of $Hf_{0.84}Ta_{0.16}Fe_{2-x}Cr_x$ ($0 \leq x \leq 0.25$) at room temperature. (b) Rietveld refinement plots of SXRD at room temperature for $Hf_{0.84}Ta_{0.16}Fe_2$. Red points and black lines represent observed and calculated profiles, respectively, and the difference between them is shown at the bottom of the graph. (c) Crystal structure (left) and Kagome layer on (001) plane (right) of $Hf_{0.84}Ta_{0.16}Fe_2$. (d) Linear thermal expansion ($\Delta L/L_0$) curves of $Hf_{0.84}Ta_{0.16}Fe_{2-x}Cr_x$ ($0 \leq x \leq 0.25$).

To clarify the changing trend of the intrinsic lattice thermal expansion, the temperature dependence of the synchrotron X-ray diffraction (SXRD) patterns of $Hf_{0.84}Ta_{0.16}Fe_2$ within the temperature range of 100 - 400 K was tested (Figure 2a). The temperature-dependent intensities of (112) and (201) peaks are specifically marked in Figure 2b. It can be roughly observed that as the temperature rises from 100 K, the

diffraction peaks of (200), (112) and (201) shift towards lower angles very slowly, but when it reaches 250 K, they suddenly jump to higher diffraction angles, and then shift towards lower diffraction angles as the temperature continues to increase. This directly reflects the lattice thermal expansion characteristics of $Hf_{0.84}Ta_{0.16}Fe_2$, that is, a short-lived and intense negative thermal expansion at a narrow temperature range around 250 K.
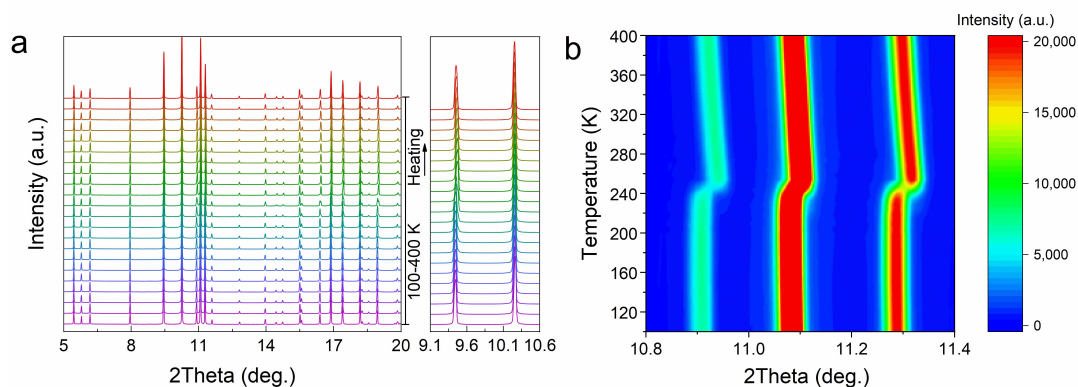
Figure 2. (a) Temperature-dependent SXRD patterns of $Hf_{0.84}Ta_{0.16}Fe_2$. (b) Temperature dependence of intensities of (200), (112), and (201) peaks in SXRD patterns.

Through the structural refinement of the SXRD data, we obtained the dependence of the lattice parameters on temperature (Figure 3a). The a-axis exhibited a relatively intense negative thermal expansion phenomenon, while the c-axis showed a positive thermal expansion. Since the positive thermal expansion occurring on the c-axis was insufficient to exceed the intense negative thermal expansion on the ab-plane, the overall volume change still demonstrated a negative thermal expansion trend (Figure 3b). This coincides with the temperature range and coefficient ratio of the macroscopic thermal expansion. It has proved the accuracy of the macroscopic thermal expansion measurements in Figure 1d.
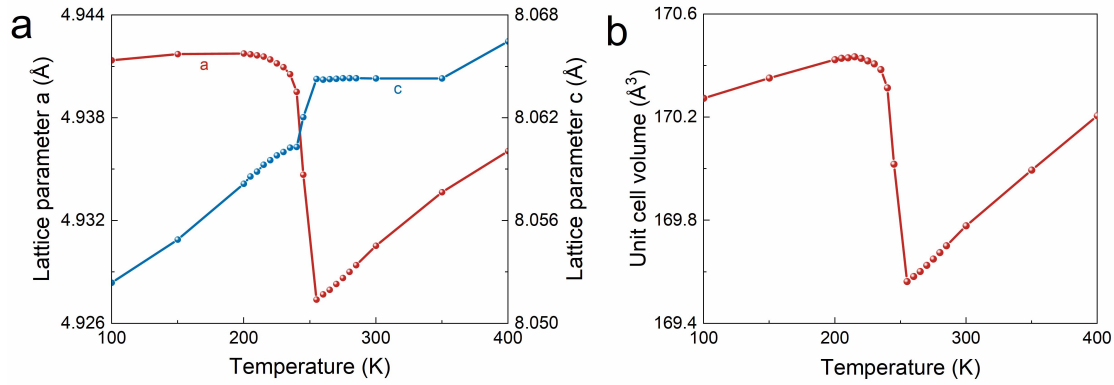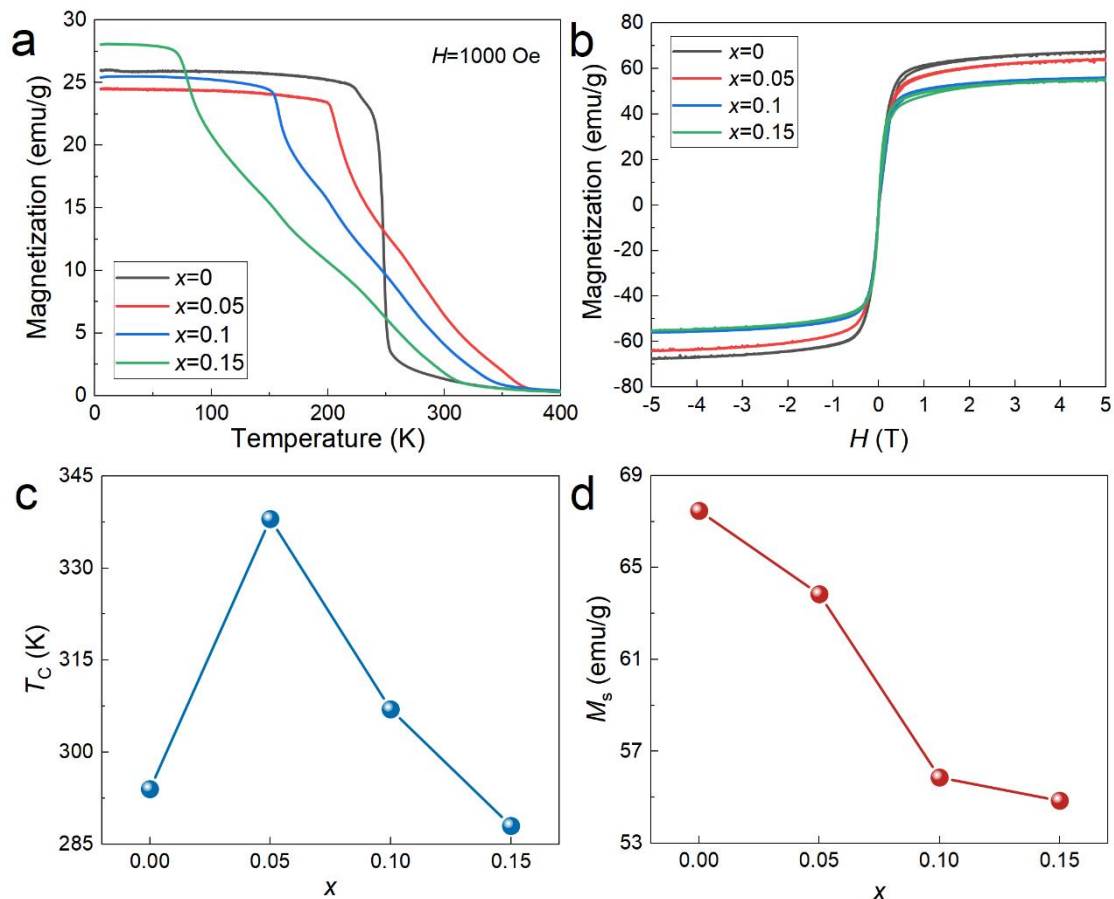
Figure 3. (a) Temperature dependence of lattice parameters a and c for $Hf_{0.84}Ta_{0.16}Fe_2$. (b) Temperature dependence of unit cell volume for $Hf_{0.84}Ta_{0.16}Fe_2$.

Furthermore, Tong has already studied that the negative thermal expansion of (Hf, Ta)Fe_2 is caused by magnetic phase transitions. Through using electron spin resonance (ESR) to study the magnetic phase transition, it has been confirmed that the negative thermal expansion of (Hf, Ta)Fe_2 is due to spontaneous volume magnetostriction[37]. Therefore, we conducted tests on the magnetism of $Hf_{0.84}Ta_{0.16}Fe_{2-x}Cr_x$ ($0 \leq x \leq 0.25$). From the magnetic field and temperature-dependent magnetization curves, we found that $Hf_{0.84}Ta_{0.16}Fe_{2-x}Cr_x$ ($0 \leq x \leq 0.25$) still ferromagnetic at low temperatures, and undergoes a phase transition to paramagnetic phase when the temperature rises, and the addition of the Cr element makes the transition from ferromagnetic to antiferromagnetic more gentle (Figure 4a). Moreover, as the Cr content increased, the saturation magnetization of all the samples decreased accordingly (Figure 4b). Meanwhile, we obtained T_C by measuring the extrapolated tangent line when the M-T curve undergoes a sudden change. This shows a good consistency compared with the T_C obtained from the Curie-Weiss fitting (Figure 4c)[38]. The lower fitting data after adding Cr may be caused by the antiferromagnetism brought by Cr. We believe that in this system, the substitution of Fe atoms by Cr atoms presents a special magnetic influence mechanism. Initially, when a small number of Cr atoms entered the lattice to carry out substitution, the antiferromagnetic characteristics carried by themselves introduced new antiferromagnetic coupling effects. To some extent, this new coupling mode optimized the magnetic interactions within the system, making the cooperative arrangement of

magnetic moments among atoms more orderly, and thus promoting the increase in the Curie temperature (T_C). However, as the amount of Cr substitution further increased, the magnetic balance within the system was disrupted. Excessive antiferromagnetic Cr atoms led to excessive disorder in the magnetic interactions, seriously destroying the original ordered arrangement of magnetic moments, and gradually weakening the overall magnetism. Eventually, the T_C dropped to some extent. At the same time, as the Cr content increased, the trend of the transition from the ferromagnetic to the paramagnetic state also became gentler from being intense. When the Cr content was 0.1, the degree of weakening of the magnetic interactions just promoted the transformation from negative thermal expansion to zero thermal expansion.

Figure 4. (a) Temperature dependence of magnetization for $Hf_{0.84}Ta_{0.16}Fe_{2-x}Cr_x$ ($0 \leq x \leq 0.15$). (b) Hysteresis loops of $Hf_{0.84}Ta_{0.16}Fe_{2-x}Cr_x$ ($0 \leq x \leq 0.15$) from -5 T to 5 T at 5 K. (c) Curie temperature (T_C) and (d) saturation magnetization (M_S) for $Hf_{0.84}Ta_{0.16}Fe_{2-x}Cr_x$ ($0 \leq x \leq 0.15$).

Furthermore, since it is known that the NTE phenomenon of $Hf_{0.84}Ta_{0.16}Fe_2$ mainly occurs in the ab plane, we need to obtain the changes in the interatomic bond lengths within the ab plane for further research. Therefore, after refining the temperature-dependent X-ray diffraction data, we obtained the bond lengths between Fe atoms. The bond lengths between Fe atoms at the 2a site and those at the 6h site did not show significant changes with the variation of temperature. However, interestingly, we found that the bond lengths between Fe atoms at the 6h site within the ab plane all decreased when the temperature rose to around 250 K (Figure 5a). Therefore, we infer that the bond length contraction between Fe atoms at the 6h position in the ab plane affects the Fe - Fe atomic interaction, which is the main reason for the NTE in $Hf_{0.84}Ta_{0.16}Fe_2$. This is also consistent with the research on the thermal expansion behavior of Kagome magnets in the ab plane of $(Hf, Ta)Fe_2$ conducted by Xu et al[35].
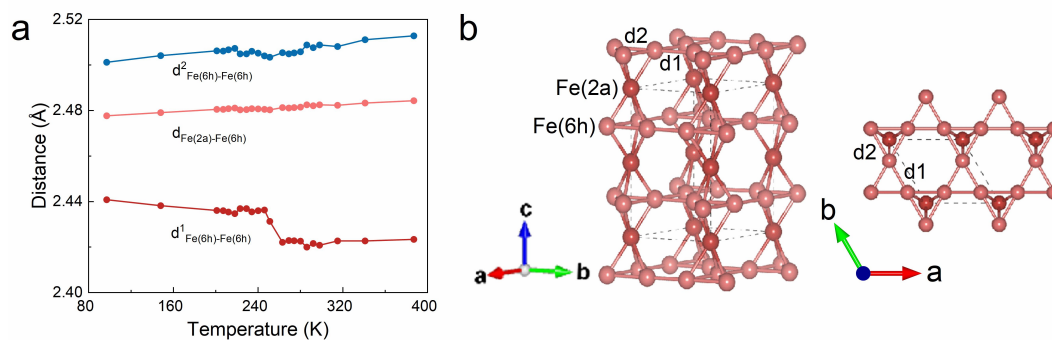
Figure 5. (a) Temperature dependence of the pair distance of different Fe - Fe pairs obtained from the refined results. (b) The position of Fe atoms and the bond lengths models of $Hf_{0.84}Ta_{0.16}Fe_2$.

In order to observe the relationship between magnetic changes and anomalous thermal expansion more intuitively, we fitted the thermal expansion curve with the curve of magnetic properties changing with temperature (Figure 6). It turned out that the result was consistent with our previous speculation. For $Hf_{0.84}Ta_{0.16}Fe_2$, as the ferromagnetic phase rapidly transformed into the paramagnetic phase (Figure 6), the thermal

expansion curve also dropped sharply at almost the same temperature point. However, in Figure 6b, the ferromagnetic phase of $Hf_{0.84}Ta_{0.16}Fe_{1.9}Cr_{0.1}$ slowly transformed into the paramagnetic phase, and correspondingly, the thermal expansion curve in the same temperature range also showed a trend of becoming gentler and exhibited a zero thermal expansion phenomenon. This simultaneously verified the strong coupling behavior between the thermal expansion behavior and the magnetic phase transition in $Hf_{0.84}Ta_{0.16}Fe_{2-x}Cr_x$ $(0 \le x \le 0.15)$[39].
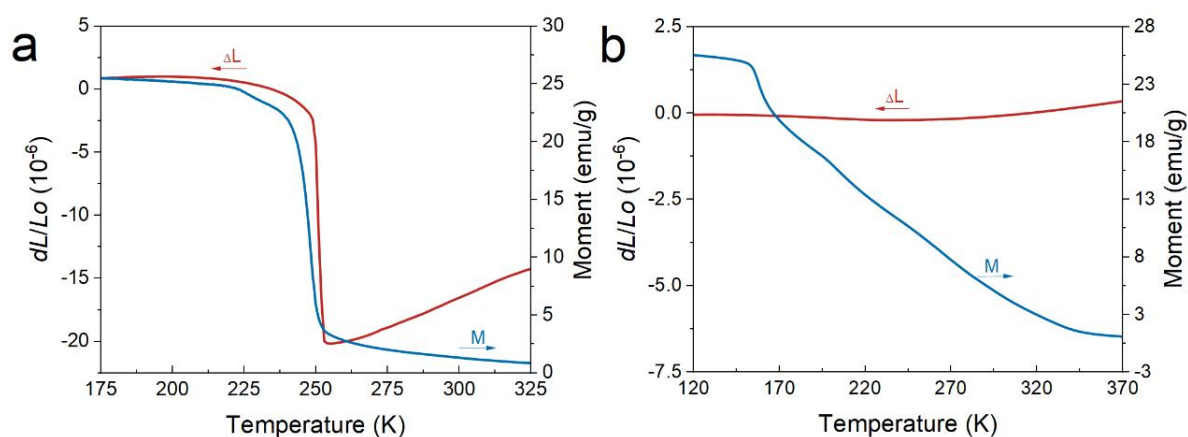
Figure 6. (a) Temperature dependence of coefficient of thermal expansion and magnetization of $Hf_{0.84}Ta_{0.16}Fe_2$. (b) Temperature dependence of coefficient of thermal expansion and magnetization of $Hf_{0.84}Ta_{0.16}Fe_{1.9}Cr_{0.1}$.

CONCLUSION

In summary, we developed a ZTE material with a thermal expansion coefficient of 1.55×10^{-6} K^{-1} and an operating temperature range covering room temperature (110 – 370 K.). Our strategy to regulate the negative thermal expansion of $Hf_{0.84}Ta_{0.16}Fe_2$ involves chemical substitution and continuous optimization composition. The strong interaction between Fe atoms drives the negative thermal expansion of $Hf_{0.84}Ta_{0.16}Fe_2$. Introducing Cr atoms weakens the magnetic interaction between Fe atoms, reducing the extent of negative thermal expansion. When the Cr content reaches 0.1, the weakened and decelerated interaction between Fe atoms in the 6h plane delays the transformation from the ferromagnetic to antiferromagnetic phase, leading to ZTE. This research expands the understanding of zero thermal expansion regulation in (Hf, Ta)Fe$_2$ and highlights the

potential applications of dimensionally stable materials over wide temperature ranges in advanced modern technologies[40].

DECLARATIONS

Acknowledgments

Author Contributions

W.X.B. fabricated the specimen. W.X.B, and A.M.J. analyzed the diffraction data, atomic structure and corresponding theories. W.X.B. conceived the study and designed the research. W.X.B and A.M.J. wrote the paper. W.X.B. and A.M.J. contributed equally to this work. All authors read and contributed to the manuscript.

Data Availability Statement

The data that support the findings of this study are available from the corresponding author upon reasonable request.

Financial support and sponsorship

Declaration of Competing Interest

The authors declare that they have no known competing financial interests or personal relationships that could have influenced the work reported in this paper.

Ethical approval and consent to participate

Not applicable.

Consent for publication

Not applicable.

Copyright

REFERENCES

1. Attfield JP. Condensed-matter physics: A fresh twist on shrinking materials. *Nature* 2011;480:465-6. [PMID:22193098 DOI:10.1038/480465a]

2. Mary TA, Evans JSO, Vogt T, Sleight AW. Negative Thermal Expansion from 0.3 to 1050 Kelvin in ZrW_2O_8. *Science* 1996;272:90-2. [DOI:10.1126/science.272.5258.90]

3. Cao Y, Lin K, Khmelevskyi S, et al. Ultrawide Temperature Range Super-Invar Behavior of $R_2(Fe,Co)_{17}$ Materials (R = Rare Earth). *Phys Rev Lett* 2021;127:055501. [DOI:10.1103/physrevlett.127.055501]

4. Nishihara Y, Yamaguchi Y. Magnetic Phase Transitions in Itinerant Electron Magnets $Hf_{1-x}Ta_xFe_2$. *J Phys Soc Jpn* 1983;52:3630-6. [DOI:10.1143/jpsj.52.3630]

5. Hu L, Chen J, Sanson A, et al. New Insights into the Negative Thermal Expansion: Direct Experimental Evidence for the "Guitar-String" Effect in Cubic ScF3. *J Am Chem Soc* 2016;138:8320-3. [DOI:10.1021/jacs.6b02370]

6. Takenaka K. Progress of Research in Negative Thermal Expansion Materials: Paradigm Shift in the Control of Thermal Expansion. *Front Chem* 2018;6:267. [PMID:30013970 DOI:10.3389/fchem.2018.00267 PMCID:PMC6036420]

7. Yokoyama T, Eguchi K. Anisotropic thermal expansion and cooperative Invar and anti-Invar effects in mn alloys. *Phys Rev Lett* 2013;110:075901. [PMID:25166383 DOI:10.1103/physrevlett.110.075901]

8. Gao Q, Sun Y, Shi N, et al. Large isotropic negative thermal expansion in water-free Prussian blue analogues of ScCo(CN)6. *Scripta Materialia* 2020;187:119-24. [DOI:10.1016/j.scriptamat.2020.05.041]

9. Yuan J, Song Y, Xing X, Chen J. Magnetic structure and uniaxial negative thermal expansion in antiferromagnetic CrSb. *Dalton Trans* 2020;49:17605-11. [DOI:10.1039/d0dt03277h]

10. Song Y, Sun Q, Xu M, et al. Negative thermal expansion in $(Sc,Ti)Fe_2$ induced by an unconventional magnetovolume effect. *Mater Horiz* 2020;7:275-81. [DOI:10.1039/c9mh01025d]

11. Lohaus SH, Heine M, Guzman P, et al. A thermodynamic explanation of the Invar effect. *Nat Phys* 2023;19:1642-8. [DOI:10.1038/s41567-023-02142-z]

12. Pang X, Song Y, Shi N, Xu M, Zhou C, Chen J. Design of zero thermal expansion and high thermal conductivity in machinable xLFCS/Cu metal matrix composites. *Composites Part B: Engineering* 2022;238:109883. [DOI:10.1016/j.compositesb.2022.109883]

13. van Schilfgaarde M, Abrikosov IA, Johansson B. Origin of the Invar effect in iron–nickel alloys. *Nature* 1999;400:46-9. [DOI:10.1038/21848]

14. Diop LV, Amara M, Isnard O. Large magnetovolume effects due to transition from the ferromagnetic to antiferromagnetic state in Hf0.825Ta0.175Fe2 intermetallic compound. *J Phys Condens Matter* 2013;25:416007. [DOI:10.1088/0953-8984/25/41/416007]

15. Chen F, Xie H, Huo M, Wu H, Li L, Jiang Z. Effects of magnetic field and hydrostatic pressure on the antiferromagnetic–ferromagnetic transition and

magneto-functional properties in Hf1-xTaxFe2 alloys. *Tungsten* 2023;5:503-11. [DOI:10.1007/s42864-022-00156-3]

16. Dong X, Lin K, Yu C, et al. Zero thermal expansion in non-stoichiometric and single-phase (Hf,Nb)Fe2.5 alloy. *Scripta Materialia* 2023;229:115388. [DOI:10.1016/j.scriptamat.2023.115388]

17. Yan-jun H, Zhong-ying J, Nan C, Zhi-da H, Shu-zhen L, Yuan-fu H. Magnetic Properties of Hf $_{0.8}$ Ta $_{0.2}$ (Fe $_{0.97}$ A $_{0.03}$) $_2$ (A=Al, Co, Mn) Systems. *Chinese Phys Lett* 2006;23:3309-12. [DOI:10.1088/0256-307x/23/12/052]

18. Duijn HGM, Brück E, Menovsky AA, et al. Magnetic and transport properties of the itinerant electron system Hf1− x Ta x Fe2. *Journal of Applied Physics* 1997;81:4218-20. [DOI:10.1063/1.365125]

19. Diop L, Isnard O, Suard E, Benea D. Neutron diffraction study of the itinerant-electron metamagnetic Hf0.825Ta0.175Fe2 compound. *Solid State Communications* 2016;229:16-21. [DOI:10.1016/j.ssc.2015.12.013]

20. Ouyang Z, Rao G, Yang H, et al. Structure and unusual magnetic properties in the itinerant electron system Hf0.8Ta0.2(Fe1−xCox)2. *Journal of Alloys and Compounds* 2004;370:18-24. [DOI:10.1016/j.jallcom.2003.08.088]

21. Cao Y, Xu Y, Khmelevskyi S, et al. Interplanar Magnetic Orders and Symmetry-Tuned Zero Thermal Expansion in Kagomé Metal (Zr,Ta)Fe $_2$. *Chem Mater* 2023;35:9167-74. [DOI:10.1021/acs.chemmater.3c01894]

22. Song Y, Chen J, Liu X, et al. Zero Thermal Expansion in Magnetic and Metallic Tb(Co,Fe)(2) Intermetallic Compounds. *J Am Chem Soc* 2018;140:602-5. [DOI: 10.1021/jacs.7b12235]

23. Huang R, Liu Y, Fan W, et al. Giant negative thermal expansion in NaZn13-type La(Fe, Si, Co)13 compounds. *J Am Chem Soc* 2013;135:11469-72. [DOI:10.1021/ja405161z]

24. Li S, Huang R, Zhao Y, Wang W, Han Y, Li L. Zero Thermal Expansion Achieved by an Electrolytic Hydriding Method in La(Fe,Si) $_{13}$ Compounds. *Adv Funct Materials* 2017;27:1604195. [DOI:10.1002/adfm.201604195]

25. Xu M, Song Y, Xu Y, et al. High-Temperature Zero Thermal Expansion in HfFe$_{2+\delta}$ from Added Ferromagnetic Paths. *Chem Mater* 2022;34:9437-45. [DOI:10.1021/acs.chemmater.2c01732]

26. Yuan X, Wang B, Sun Y, et al. High-Entropy Anti-Perovskites with Enhanced Negative Thermal Expansion Behavior. *Adv Funct Materials* 2024;34:2404629. [DOI:10.1002/adfm.202404629]

27. Song Y, Chen J, Liu X, et al. Structure, Magnetism, and Tunable Negative Thermal Expansion in (Hf,Nb)Fe$_2$ Alloys. *Chem Mater* 2017;29:7078-82. [DOI:10.1021/acs.chemmater.7b02563]

28. Cen D, Wang B, Chu R, et al. Design of (Hf,Ta)Fe2/Fe composite with zero thermal expansion covering room temperature. *Scripta Materialia* 2020;186:331-5. [DOI:10.1016/j.scriptamat.2020.05.048]

29. Bag P, Rawat R, Chaddah P, Babu PD, Siruguri V. Unconventional thermal effects across first-order magnetic transition in the Ta-doped HfFe2 intermetallic. *Phys Rev B* 2016;93. [DOI:10.1103/physrevb.93.014416]

30. Li B, Luo XH, Wang H, et al. Colossal negative thermal expansion induced by magnetic phase competition on frustrated lattices in Laves phase compound (Hf,Ta)Fe2. *Phys Rev B* 2016;93. [DOI:10.1103/physrevb.93.224405]

31. Qiao Y, Song Y, Lin K, et al. Negative Thermal Expansion in (Hf,Ti)Fe(2) Induced by the Ferromagnetic and Antiferromagnetic Phase Coexistence. *Inorg Chem* 2019;58:5380-3. [DOI:10.1021/acs.inorgchem.8b03600]

32. Wada H, Shimamura N, Shiga M. Thermal and transport properties of Hf1-xTaxFe2. *Phys Rev B Condens Matter* 1993;48:10221-6. [PMID:10007298 DOI:10.1103/physrevb.48.10221]

33. Delyagin N, Erzinkyan A, Parfenova V, Rozantsev I, Ryasny G. Ferromagnetic-to-antiferromagnetic transition in (Hf1−xTix)Fe2 intermetallic compounds induced by geometrical frustration of the Fe(2a) sites. *Journal of Magnetism and Magnetic Materials* 2008;320:1853-7. [DOI:10.1016/j.jmmm.2008.02.149]

34. Sun Y, Cao Y, Hu S, et al. Interplanar Ferromagnetism Enhanced Ultrawide Zero Thermal Expansion in Kagome Cubic Intermetallic (Zr,Nb)Fe(2). *J Am Chem Soc* 2023;145:17096-102. [DOI:10.1021/jacs.3c03160]

35. Xu J, Wang Z, Huang H, et al. Significant Zero Thermal Expansion Via Enhanced Magnetoelastic Coupling in Kagome Magnets. *Adv Mater* 2023;35:e2208635. [DOI:10.1002/adma.202208635]

36. Diop LVB, Kastil J, Isnard O, Arnold Z, Kamarad J. Collapse of ferromagnetism in itinerant-electron system: A magnetic, transport properties, and high pressure study of (Hf,Ta)Fe2 compounds. *Journal of Applied Physics* 2014;116:163907. [DOI:10.1063/1.4900034]

37. Li L, Tong P, Zou Y, et al. Good comprehensive performance of Laves phase Hf1-Ta Fe2 as negative thermal expansion materials. *Acta Materialia* 2018;161:258-65. [DOI:10.1016/j.actamat.2018.09.029]

38. Chen J, Hu L, Deng J, Xing X. Negative thermal expansion in functional materials: controllable thermal expansion by chemical modifications. *Chem Soc Rev* 2015;44:3522-67. [PMID:25864730 DOI:10.1039/c4cs00461b]

39. Qiao Y, Liaquat I, Zhu Y, Guo J, Liang E, Gao Q. Tunable thermal expansion via the magnetic phase competition in kagome magnets. *Applied Physics Letters* 2024;125:032403. [DOI:10.1063/5.0218339]

40. Wang H, Wang Y, Gong Y, et al. Designing (Hf,Ta)Fe2-based zero thermal expansion composites consisting of multiple Laves phases. *Rare Met* 2024;43:6596-605. [DOI:10.1007/s12598-024-02867-7]